WAVE-INDUCED SEEPAGE EFFECTS ON A VERTICAL CYLINDER

by

Thomas J.P. Durand[1] and Peter L. Monkmeyer[2], M. ASCE

ABSTRACT

This study deals with the seepage effects experienced by a large, vertical, circular cylinder resting on a submerged bed of sand when planar water waves interact with it. Potential theory is used to describe the seepage flow field. The sea bottom pressure condition is determined from the water field velocity potential derived by MacCamy and Fuchs (1954) in the case of planar waves diffracted by a large impervious cylinder. Consideration is also given to cylinders with a thin circular base whose diameter exceeds that of the cylinder itself.

The problem formulation as well as the initiation of the analysis apply to the general case of a bed of sand with finite depth.

For the case of infinite depth of the porous medium, theoretical solutions for the seepage pressure are obtained in the form of infinite integrals. Theoretical solutions for the pressure along the cylinder circular base are then derived, leading by integration to closed form expressions for the wave-induced seepage uplift force and overturning moment exerted on the cylinder. These expressions for the force and moment, which are presented in non-dimensional form are shown to be universal functions of a unique variable. Graphs are provided so that very few computations are required to determine the uplift force and overturning moment exerted on a cylinder. A comparison with various approximate theories reveals the present theory to be the only one which gives reliable results in general.

The amplitude and phase angle of the oscillating wave-induced pressure along the cylinder base are determined numerically. Results for the pressure amplitude are presented as non-dimensional ratios to the amplitude of the pressure that would prevail if no cylinder were disturbing the wave field.

Expressions for the exit gradient around the cylinder base are also determined. Contours of the ratio of the exit gradient to the one that would prevail in the absence of a cylinder are presented.

Laboratory measurements of uplift pressure amplitudes on a circular cylinder show good agreement with theoretical calculations.

INTRODUCTION

The rapid development of offshore construction in recent years has led to some complex technological problems, not the least of which are those concerned with the foundation and the possibility of foundation

---

1 Research Assistant, Department of Civil and Environmental Engineering, University of Wisconsin, Madison, Wisconsin 53706

2 Professor of Civil and Environmental Engineering, University of Wisconsin, Madison, Wisconsin 53706

failure. There is some indication that such failure may be due to wave-induced seepage in the porous sea bed. Dynamic seepage pressures are believed to induce erosion phenomenon around the foundation of some structures as well as the cyclic uplift forces which act on the underside of a structure resting on the sea bottom. As a result, research dealing with the dynamics of wave-induced seepage in sea beds has been conducted by a number of investigators.

Most of the past research on the subject has focused upon the mathematical formulation required to obtain a realistic model of the physical phenomenon involved. Although work on this matter is still in progress, it may be useful to summarize the assumptions and governing equations used by some of the contributors. Sleath (1970) performed experiments which strongly support Putnam's (1949) use of potential theory, thereby suggesting that elastic effects can be neglected. Later, however, Moshagen and Tørum (1975), by including a water compressibility term in the continuity equation, derived a "heat conduction type" equation for the pressure. In the case of coarse sand, solutions to their equation approach those of Putnam, using potential theory, asymptotically. The results deviate only slightly for fine sands and are quite different for silts and silty clays. Yamamoto (1977), using the consolidation theory of Biot (1941), derived and solved a system of partial differential equations taking into account the compressibility of the water and the skeleton. Interestingly enough his solutions are very similar to those obtained from potential theory in the case of coarse sands and slightly different in the case of fine sands. Madsen (1978) also considered compressibility of water and skeleton as well as other soil properties. He concluded that for fine sands, as well as coarse sands which are isotropic, the effect of compressibility of fluid and skeleton is negligible.

It should be emphasized that all the previously mentioned studies apply only to planar waves unaffected by any structure. No consideration was given to the presence of a structure until Moshagen and Monkmeyer (1979) completed an investigation in which an embedded vertical cylinder was subjected to horizontal, wave-induced seepage forces. For a more detailed literature review the reader is referred to their paper.

The objective of this study is to analyze the dynamic seepage pressures and forces exerted on the base of a single, vertical, circular cylinder resting on a bed of sand when linear progressive waves interact with it. The cylinder does not penetrate the sea bed but its base can have a larger radius than the cylinder body itself. This extended circular base, when it is considered, is assumed to be infinitely thin. (See Fig. 1.)

The good agreement among the solutions of the various theories mentioned previously, when applied to sands (especially coarse sands), together with the great simplification it provides, makes potential theory the logical choice for the present study, especially in view of Sleath's experimental confirmation. The coupling condition between the sea water field and the pore water seepage field is obtained by means of a pressure matching procedure along the sea bottom. To accomplish

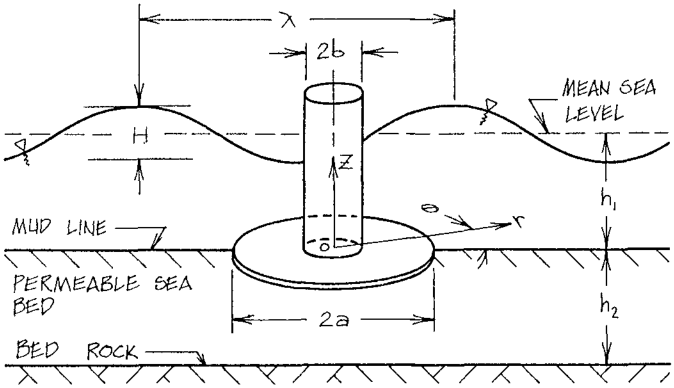

Fig. 1. Definition Sketch

this, MacCamy and Fuchs' (1954) potential function, describing both the incident and diffracted waves of the sea water flow field, is used to derive an analytic expression for the sea water pressure on the sea bottom. This pressure distribution provides a coupling boundary condition for the dynamic seepage field. The various additional boundary conditions are also stated for the seepage potential function. Although the analysis is initiated for the general case of a porous medium of finite thickness, theoretical solutions for the seepage pressures in the sea bed are only presented for the case of a porous medium of infinite thickness. Indeed, only in that case do the solutions lead to relatively simple expressions for the pressure distribution along the underside of the cylinder base. The uplift force and overturning moment exerted on the cylinder base by the dynamic seepage can then be obtained by integration.

THEORETICAL ANALYSIS

Governing Equation

The seepage flow field in the porous medium is assumed to follow Darcy's law,

$$\vec{q} = \nabla\phi_2 \tag{1}$$

with

$$\phi_2 = -K[p_2/\gamma + z] \tag{2}$$

where ϕ_2 = velocity potential $[L^2/T]$

γ = specific weight of water $[M/L^2T^2]$

p_2 = pressure $[M/LT^2]$

$\vec{q}$ = specific discharge $[L/T]$

K = hydraulic conductivity $[L/T]$

z = vertical coordinate $[L]$

Assuming a completely saturated soil and neglecting the various effects due to the compressibilities of the water, porous skeleton and sand grains themselves, the continuity equation takes the form:

$$\nabla \cdot \vec{q} = 0 \tag{3}$$

By substitution of Eq. 1 into Eq. 3, the governing equations for seepage then lead to Laplace's Equation,

$$\nabla^2 \phi_2 = 0 \tag{4}$$

so that under the assumption of essentially incompressible water flowing through a saturated, rigid, isotropic porous medium, potential theory may be used to describe the seepage flow field, as noted before.

Boundary Conditions

In order to couple the sea water field to the seepage flow field, the pore water pressure distribution along the mud line is matched to the corresponding sea water pressure distribution. To this end, use is made of the well-known MacCamy and Fuchs (1954) velocity potential for small amplitude water waves diffracted by a vertical circular cylinder of radius b.

$$\phi_1(r,\theta,z,t) = \frac{gH}{2\omega} e^{-i\omega t} \frac{\cosh(kz)}{\cosh(kh_1)} \sum_{m=0}^{\infty} \frac{\varepsilon_m i^m C_m(kr)}{H_m^{(1)'}(kb)} \cos(m\theta) \tag{5}$$

where $C_m(kr) = J_m'(kb)\, H_m^{(1)}(kr) - H_m^{(1)'}(kb)\, J_m(kr)$

$$\varepsilon_m = \begin{cases} 1 & \text{if } m = 0 \\ 2 & \text{if } m \geq 1 \end{cases}$$

and where
g = acceleration due to gravity $[L/T^2]$
H = wave height $[L]$
ω = $2\pi/T$ = wave frequency = $[gk \tanh(kh_1)][T^{-1}]$
k = wave number $[L^{-1}]$
h_1 = elevation of mean sea level above sea bottom $[L]$
b = cylinder radius $[L]$
$J_m(\ )$ = Bessel function of the first kind of order m
$H_m^{(1)}(\ )$ = Hankel function of the first kind of order m

where the primes indicate differentiation with respect to the argument. It should be emphasized at this point that MacCamy and Fuchs' velocity potential is valid for cylinders large with respect to the wave dimensions. More specifically, since the MacCamy and Fuchs theory neglects drag but considers inertial effects it is only valid when drag effects are minimal. As Dean and Harleman (1966) point out, this is the case when H/b is small and kh_1 is large.

By substituting Eq. 5 into the linearized dynamic pressure equation,

$$\frac{\partial \phi_1}{\partial t} + \frac{p_1}{\rho} = 0 \tag{6}$$

where ρ = mass density $[M/L^3]$,

one can derive an expression for the dynamic pressure at the bottom of the sea. The next step is to equate the pore water pressure immediately below the mud line to the corresponding sea water pressure immediately above.

$$p_1 = p_2 \qquad \text{at } z = 0 \qquad \text{for } r \geq a \tag{7}$$

where a = radius of the cylinder circular base [L].

Making use of Eq. 2 one finally obtains the following condition for ϕ_2 along the mud line

$$\phi_2 = \frac{K}{g}\frac{\partial \phi_1}{\partial t} = -\frac{iK}{g}\omega\phi_1 \qquad \text{at } z = 0 \quad r \geq a$$

or, henceforth dropping the subscript 2,

$$\phi(r \geq a, \theta, z=0, t) = -i\,\frac{KH\,e^{-i\omega t}}{2\cosh(kh_1)} \sum_{m=0}^{\infty} \frac{\varepsilon_m i^m C_m(kr)}{H_m^{(1)\prime}(kb)} \cos(m\theta) \tag{8}$$

The impervious condition at bed rock is

$$\frac{\partial \phi}{\partial z} = 0 \qquad \text{at } z = -h_2 \tag{9}$$

while the impervious condition along the circular disc of radius a on the underside of the base of the structure is

$$\frac{\partial \phi}{\partial z} = 0 \qquad \text{at } z = 0 \qquad r \leq a \tag{10}$$

It should be noted that the radiation condition associated with the present potential problem - such a condition is needed to insure the uniqueness of the solution - turns out to be implicitly integrated in the pressure matching condition along the mud line so that no additional requirement need be prescribed.

The governing Laplace equation, Eq. 4, is therefore constrained by its boundary conditions, Eqs. 8, 9 and 10. It clearly appears that a Neumann type condition and a Dirichlet type condition are prescribed on different parts of the same boundary, namely the upper plane z = 0, so that the potential problem to be solved is of the mixed boundary value type.

Solution

Due to the non-axisymmetric diffracted wave pattern, the analysis is initiated in three dimensions using a non-dimensional coordinate system

$$r^* = r/a \qquad z^* = z/a \qquad h_2^* = h_2/a \tag{11}$$

The stars are dropped for simplicity of the notation.

The particular form of the pressure matching condition, Eq. 8, suggests that the unknown potential function be expressed in a Fourier expansion of the polar angle,

$$\phi(r,\theta,z,t) = -i\,\frac{KH\,e^{-i\omega t}}{2\cosh(kh_1)}\sum_{m=0}^{\infty}\frac{\varepsilon_m i^m\,\phi_m(r,z)}{H_m^{(1)'}(kb)}\cos(m\theta) \tag{12}$$

where the functions $\phi_m(r,z)$ are the new problem unknowns satisfying the reduced partial differential equation

$$\frac{\partial^2\phi_m}{\partial r^2} + \frac{1}{r}\frac{\partial\phi_m}{\partial r} - \frac{m^2}{r^2}\phi_m + \frac{\partial^2\phi_m}{\partial z^2} = 0 \tag{13}$$

A solution of Eq. 13, satisfying the bed rock condition, Eq. 9, can be obtained through a Hankel integral transform and is given by

$$\phi_m(r,z) = \int_0^{\infty} pA_m(p)\,[e^{pz} + e^{-p(z+2h_2)}]\,J_m(pr)\,dp \tag{14}$$

where $A_m(\ )$ is a new unknown function which can be determined by making use of the remaining boundary conditions, Eqs. 8 and 10,

$$\begin{aligned}&\int_0^{\infty} p\,\tanh(ph_2)\,F_m(p)\,J_m(pr)\,dp = 0 && 0\le r\le 1\\ &\int_0^{\infty} F_m(p)\,J_m(pr)\,dp = C_m(kar) && 1\le r\end{aligned} \tag{15}$$

where

$$F_m(p) = pA_m(p)\,[1 + e^{-2ph_2}] \tag{16}$$

Eqs. 15 are known as Dual Integral Equations. They obviously result from the mixed nature of the boundary value problem. Sneddon (1966) presents a thorough treatment of these equations. Closed form solutions of Dual Integral Equations have been obtained in the case of $h_2 \to \infty$, which corresponds to the physical case of infinite depth of the porous medium, and therefore this analysis will be restricted to the infinite depth case only.

For $h_2 \to \infty$, Sneddon reports Titchmarsh's solution as

$$pA_m(p) = -\sqrt{\frac{2p}{\pi}}\int_1^{\infty} t^{m+1/2}J_{m+1/2}(pt)\,dt\,\frac{d}{dt}\int_t^{\infty}\frac{C_m(kau)\,du}{u^{m-1}\sqrt{u^2-t^2}} \tag{17}$$

which, after some rearrangement and then substitution into Eq. 14, leads to

$$\phi_m(r,z) = \int_0^{\infty}\sqrt{kap}\;e^{pz}J_m(pr)\,dp\int_1^{\infty} tJ_{m+1/2}(pt)\,C^*_{m+1/2}(kat)\,dt \tag{18}$$

where

$$C^*_{m+1/2}(kat) = J'_m(kb)\, H^{(1)}_{m+1/2}(kat) - H^{(1)'}_m(kb)\, J_{m+1/2}(kat) \tag{19}$$

It should be pointed out that Eq. 18 together with Eq. 12 provide an exact expression for the wave-induced potential distribution throughout the entire seepage field when a cylinder is resting on a bed of sand of infinite thickness.

Although some simplifications of Eq. 18 can be performed by making use of the Hankel inversion formula and of a known indefinite integral for the inner integral, this would only apply for the Bessel function of first kind, $J_m(\ )$, but not for $H^{(1)}_m(\ )$ so that no equation for ϕ_m, more suited to computational purposes, could be derived.

RESULTS OF THE THEORETICAL ANALYSIS

Pressure Distribution along the Cylinder Base

Substituting z = 0 in Eq. 18, inverting the order of integration, and performing the inner integration leads to

$$\phi_m(r \le 1, 0) = \sqrt{\frac{2ka}{\pi}}\; r^m \int_1^\infty \frac{C^*_{m+1/2}(kat)\,dt}{t^{m-1/2}\sqrt{t^2-r^2}} \tag{20}$$

which can in turn be transformed into

$$\phi_m(r \le 1, 0) = C_m(kar) - \sqrt{\frac{2ka}{\pi}}\; r^m \int_r^1 \frac{C^*_{m+1/2}(kat)\,dt}{t^{m-1/2}\sqrt{t^2-r^2}} \tag{21}$$

Hence the exact solution for the wave-induced pressure distribution along the circular base of the cylinder is, dropping the hydrostatic term,

$$p(r \le 1, \theta, 0, t) = \frac{\gamma H\, e^{-i\omega t}}{2\cosh(kh_1)} \sum_{m=0}^{\infty} \frac{\varepsilon_m\, i^{m+1}\, \phi_m(r,0)}{H^{(1)'}_m(kb)} \cos(m\theta) \tag{22}$$

where, for computational purposes, Eq. 21 is transformed into

$$\phi_m(r \le 1, 0) = C_m(kar) - \sqrt{\frac{2kar}{\pi}} \int_0^{\cosh^{-1}(\frac{1}{r})} \frac{C^*_{m+1/2}(kar\cosh u)}{(\cosh u)^{m-1/2}}\, du \tag{23}$$

Tabulated numerical results for the wave-induced dynamic pressure amplitude along the cylinder base are presented as non-dimensional ratios to the amplitude of the pressure that would prevail if no cylinder were disturbing the wave field, namely

$$p_{LT} = \frac{\gamma H}{2 \cosh(kh_1)} \tag{24}$$

Hence only the infinite sum in Eq. 22 is tabulated. Table I shows the values of these pressure ratios for ka = kb = 0.2, 1.0 and ka = 2kb = 2.0.

Table I

DIMENSIONLESS PRESSURE AMPLITUDE ON THE CYLINDER BASE

ka = kb = 0.2	r/a = 0.2	r/a = 0.4	r/a = 0.6	r/a = 0.8	r/a = 1.0
θ = 0°	.85260	.85978	.87580	.90536	.99894
θ = 30°	.85285	.85979	.87500	.90288	.99067
θ = 60°	.85369	.86052	.87450	.89949	.97643
θ = 90°	.85525	.86321	.87782	.90283	.97724
θ = 120°	.85728	.86779	.88568	.91518	1.00101
θ = 150°	.85905	.87233	.89420	.92962	1.03179
θ = 180°	.85976	.87423	.89789	.93599	1.04562

ka = kb = 1.0	r/a = 0.2	r/a = 0.4	r/a = 0.6	r/a = 0.8	r/a = 1.0
θ = 0°	.33957	.25847	.26442	.40492	.88819
θ = 30°	.35685	.28891	.27930	.36903	.74425
θ = 60°	.40360	.38152	.39463	.46184	.73888
θ = 90°	.46534	.50802	.58878	.73176	1.17128
θ = 120°	.52368	.62174	.75669	.95830	1.52487
θ = 150°	.56391	.69448	.85453	1.07523	1.67346
θ = 180°	.57809	.71879	.88496	1.10795	1.70708

ka = 2kb = 2.0	r/a = 0.2	r/a = 0.4	r/a = 0.6	r/a = 0.8	r/a = 1.0
θ = 0°	.05838	.10355	.22347	.40757	.92881
θ = 30°	.06704	.09116	.18303	.33408	.78076
θ = 60°	.09431	.11759	.19394	.34493	.83519
θ = 90°	.13022	.18857	.30615	.52746	1.27124
θ = 120°	.16014	.23754	.36243	.58202	1.38303
θ = 150°	.17771	.25566	.35972	.52815	1.21639
θ = 180°	.18326	.25908	.35205	.49587	1.11703

Uplift Force and Overturning Moment on the Structure

In addition to providing a simplifying transformation, the Fourier expansion, as performed at the beginning of the analysis, also has the well-known advantage of extracting from the pressure the very terms required for calculating the uplift force and overturning moment exerted on the cylinder base. More specifically, when performing the integration of the pressure, only the zero or first order terms of the Fourier infinite series make a non-zero contribution to the force or moment respectively. Furthermore, in both cases, the corresponding integration of Eq. 21 involves two integrations which can be inverted and performed analytically. Various straightforward algebraic manipulations - for the detailed derivation see Durand (1978) - finally yield closed form expressions for the wave-induced seepage uplift force and overturning moment exerted on the cylinder base as follows:

$$F = \frac{\gamma H}{\cosh(kh_1)} \frac{\pi a^2}{ka} A_o(kb) \cos(\omega t + \alpha_o(kb))$$

$$\{J_1(kb)[Y_1(ka) + \frac{2}{\pi}\frac{\cos ka}{ka} + \frac{2}{\pi} \sin ka]$$

$$-Y_1(kb)[J_1(ka) - \frac{2}{\pi}\frac{\sin ka}{ka} + \frac{2}{\pi} \cos ka]\} \tag{25}$$

$$M_o = -\frac{\gamma H}{\cosh(kh_1)} \frac{\pi a^3}{ka} A_1(kb) \sin(\omega t + \alpha_1(kb))$$

$$\{J_1'(kb)[Y_2(ka) - \frac{4}{3\pi}(\cos ka(1 - \frac{3}{(ka)^2}) - \frac{3 \sin ka}{ka}]$$

$$-Y_1'(kb)[J_2(ka) + \frac{4}{3\pi}(\sin ka(1 - \frac{3}{(ka)^2}) + \frac{3 \cos ka}{ka}]\} \tag{26}$$

where

$$\tan[\alpha_i(kb)] = \frac{Y_i'(kb)}{J_i'(kb)} \qquad i = 0,1 \tag{27}$$

$$A_i(kb) = [J_i'(kb)^2 + Y_i'(kb)^2]^{-1/2} \qquad i = 0,1 \tag{28}$$

It should be noted that Eq. 26 can be simplified when $kb = ka$ by making use of the identity,

$$J_1'(ka)\, Y_2(ka) - Y_1'(ka)\, J_2(ka) = -\frac{2}{\pi(ka)^2} \tag{29}$$

Eq. 25 may be normalized with expressions for the amplitude of the force based on two approximate theories. First, assuming that the oscillating pressure has the same amplitude and phase across the cylinder base, one obtains (see curve A in Fig. 2)

$$F_{LT_1} = \frac{\gamma H}{2 \cosh(kh_1)} \pi a^2 \tag{30}$$

The second approximate force is derived by taking into account the spatial variation of the pressure that would prevail across the cylinder base if no cylinder were present, (see curve B in Fig. 2)

$$F_{LT_2} = \frac{\gamma H}{\cosh(kh_1)} \pi a^2 \frac{J_1(ka)}{ka} \tag{31}$$

Eq. 26 may also be normalized with an approximate expression for the amplitude of the moment derived for conditions similar to those of Eq. 31. (The moment vanishes for the conditions of Eq. 30.)

$$M_{o_{LT}} = \frac{\gamma H}{\cosh(kh_1)} \pi a^3 \frac{J_2(ka)}{ka} \tag{32}$$

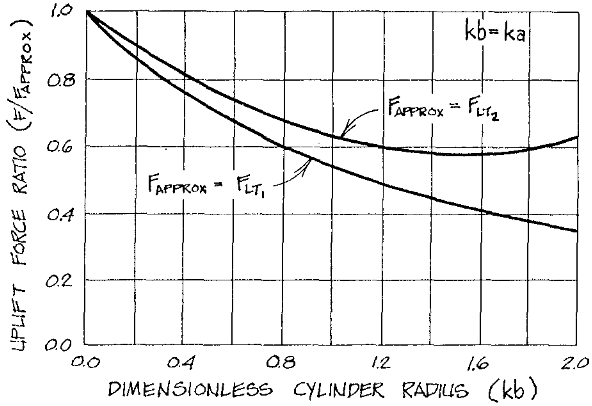

Fig. 2. Uplift Force Ratios

The ratios of the amplitude of the uplift force and overturning moment to the above normalizing quantities are plotted in Figs. 3 and 4 with ka as the variable and kb as parameter. For the most common case of a = b, each result is restricted to a universal graph because the above ratios are universal functions of a unique variable, ka.

Vertical Velocity Distribution along the Mud Line

It is important to note that Sneddon (1966) provides an alternate method to derive Eq. 20 directly from the Dual Integral Equations themselves. Interestingly enough he also provides a direct solution for the vertical velocity $\frac{\partial \phi}{\partial z}$ at the mud line through an expression for $\frac{\partial \phi_m}{\partial z}$ $(r > 1,\ z = 0)$ which can take the form

$$\frac{\partial \phi_m}{\partial z}\ (r > 1,\ z = 0) = ka\ C_m(kar) + \sqrt{\frac{2ka}{\pi}}\ r^{-m} \int_0^1 \frac{u^{m+3/2}\, C^*_{m+1/2}(kau)}{(r^2 - u^2)^{3/2}}\, du \quad (33)$$

Hence Eqs. 12 and 33 enable one to determine the vertical component of the specific discharge along the mud line and therefore the exit gradient. This quantity obviously appears to become infinite at the end of the cylinder base, r = a, but one may extract the singularity from Eq. 33 as

$$\sqrt{\frac{2ka}{\pi}}\ \frac{C^*_{m+1/2}(ka)\ r^{-m-1}}{\sqrt{r^2 - 1}} \quad (34)$$

so that the singularity of the seepage velocity field is clearly of the same weak nature as the well-known seepage velocity singularity occurring at the toe of an impervious dam resting on the top of a porous medium.

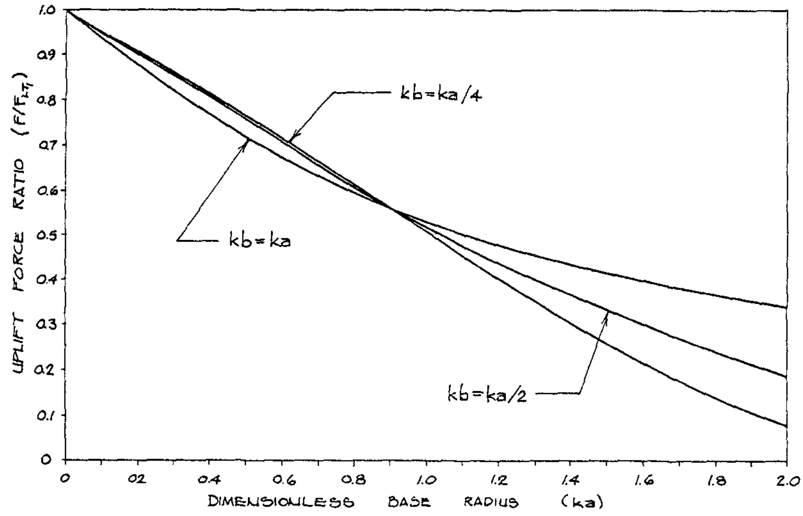

Fig. 3.a. Uplift Force Ratio: ka ≤ 2.0

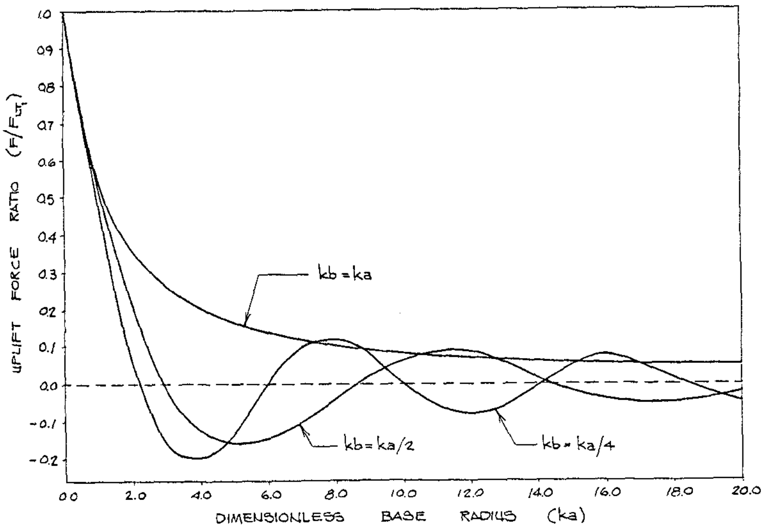

Fig. 3.b. Uplift Force Ratio: ka ≤ 20.0

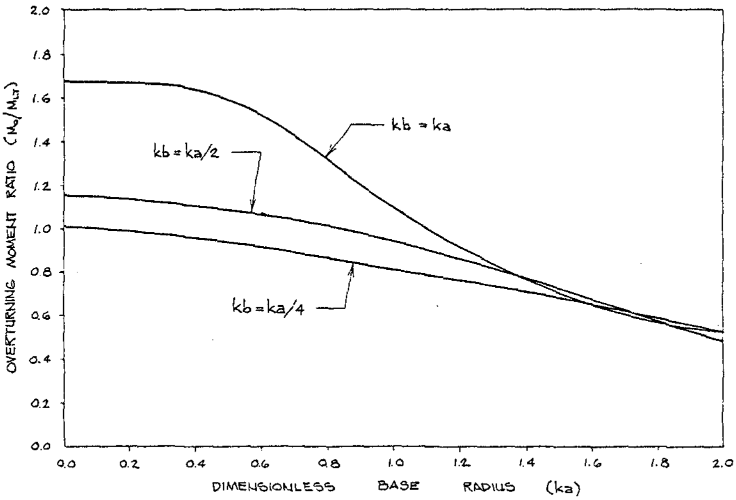

Fig. 4. Overturning Moment Ratio

The vertical component of the specific discharge can then be obtained from Eq. 12 so that the exit gradient

$$I_e = \frac{1}{K} \frac{\partial \phi}{\partial z} (r>1, \theta, 0, t) \tag{35}$$

is

$$I_e = - \frac{kH\, e^{-i\omega t}}{2 \cosh(kh_1)} \sum_{m=0}^{\infty} \frac{\varepsilon_m i^{m+1}}{kaH_m^{(1)'}(kb)} \frac{\partial \phi_m}{\partial z} (r>1, 0) \cos(m\theta) \tag{36}$$

One may use the notion of critical gradient by comparing the amplitude of the oscillating exit gradient as given by Eq. 36 to the well-known expression

$$I_{cr} = \frac{\gamma'}{\gamma_w} = \frac{S_s - 1}{1 + e} \tag{37}$$

which for sands is approximately equal to 1.

If no cylinder were disturbing the wave field, the amplitude of the exit gradient to be used in place of Eq. 36 would simply be

$$I_e = \frac{kH}{2 \cosh(kh_1)}$$

so that it appears to be useful to simply compute the quantity

$$S(r,\theta) = \left| \sum_{m=0}^{\infty} \frac{\varepsilon_m i^{m+1}}{H_m^{(1)'}(kb)} \frac{1}{ka} \frac{\partial \phi_m}{\partial z} (r>1, 0) \cos(m\theta) \right|$$

after substituting from Eq. 33.

A stability condition is then given by

$$\frac{kH}{2\cosh(kh_1)}\ S(r,\theta) \leq I_{cr} = \frac{S_s - 1}{1 + e} \simeq 1$$

in which the cylinder effect has been concentrated in a single coefficient, $S(r,\theta)$.

EXPERIMENTAL STUDY

In order to check the validity of the above theory, actual uplift pressure amplitudes along the base of a rigidly fixed, vertical, circular cylinder resting on a bed of sand were measured in the wave tank of the Hydraulics Laboratory of the University of Wisconsin-Madison. The sand used in the experiments was a fairly uniform coarse sand (about 1 mm in diameter). Although the depth of the porous medium had to be finite, it was kept large enough with respect to the wave length to permit the use of infinite-depth theory. More specifically the quantity kh_2 was equal to 2.1 so that $\tanh(kh_2)$ was close to 1, or more precisely 0.97. The tank used was 26 ft (7.92 m) long, 4 ft (1.22 m) wide and 2 ft (61 cm) deep but the inclusion of a bed of sand reduced the depth to 1 ft (30.5 cm). The sinusoidal progressive waves generated were in the following approximate ranges

$.7\ s \leq T \leq .9\ s$	$2.4' \leq L \leq 3.5'$	$2.2'' \leq H \leq 2.85''$
	(73.2 cm) (106.7 cm)	(5.59 cm) (7.24 cm)

Pressure measurements were made on the underside of the base of a vertical, circular cylinder mounted in the tank on top of the sand bed. Only one cylinder having a diameter of 5.72 in (14.5 cm) was tested with a sea water depth of 8 in (20.3 cm). A Pace transducer was used to measure pressures along the underside of the cylinder base at r_1 = .991 in (2.52 cm) and r_2 = 1.963 in (4.99 cm) while variation of the polar angle θ was obtained by rotation of the cylinder. The cylinder base had the same radius as the cylinder itself: $b = a$. See Fig. 5.

The measured pressures were normalized with respect to the pressure that would have prevailed if no cylinder had been disturbing the incoming waves. To this end, the normalizing quantities were determined by substituting the physical values into Eq. 24.

Spring and Monkmeyer (1975) studied the effect of wall confinement on pressure measurements along a cylinder placed in a tank of finite width. Correction coefficients resulting from their theoretical analysis of confinement were also used. In all cases, however, this coefficient turned out to be very close to 1 because their results and recommendations had made it possible to avoid those very parameter values based on wave length, tank width, cylinder radius for which confinement effects are important.

In Table II typical laboratory results are compared with the theory. The non-dimensional theoretical results were computed from

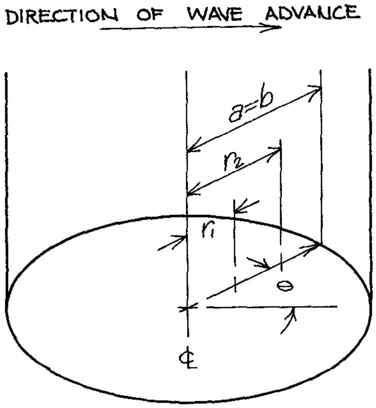

Fig. 5. Position of the Pressure Taps

Eqs. 22, 23 and 24. In combination with two values for r, r_1 and r_2, five values for the polar angle θ were used.

DISCUSSION

Table I clearly shows that the maximum pressure amplitude generally occurs at r = a, θ = 180° while the minimum is generally found at θ = 0°, between r = 0.0 and r = 0.4a. For small values of ka = kb (cylinder radius small with respect to the wave length) the maximum pressure amplitude is only 1.2 times the minimum so that the pressure amplitude variation across the cylinder base is not very significant in this case. For larger values of ka, e.g. ka = kb = 1.0, however, the maximum amplitude may be as much as 7 times larger than the minimum and 1.7 times larger than the value expected if no cylinder were disturbing the incoming wave field. A strong damping effect is also demonstrated by the small value of the amplitude of the oscillating pressure at the point of minimum pressure amplitude (about 25% of the expected value at that point if no cylinder were there). For the same cylinder, kb = 1.0, with an extended base, ka = 2.0, the pressure amplitudes around the edge of the base are not as affected by the diffracted waves as they are in the immediate vicinity of the cylinder wall, e.g. when ka = kb. However the damping effect taking place across the extended base is more striking.

Typically the value of the parameter ka for conditions corresponding to large oil tanks in the North Sea (2a = 100 m) with the century wave (L = 320 m) is about 1.0. Interestingly it was found that for values of ka of order 1, the pressure amplitude variation across the cylinder base is quite significant.

The graphs presented on Figs. 3 and 4 show how the pressure variation across the cylinder base affects the uplift force and overturning

TABLE II

COMPARISON OF SELECTED EXPERIMENTAL PRESSURE RATIOS
WITH PRESSURE RATIOS PREDICTED BY THEORY

	Experimental Data			Theory
kb (=ka)	r/a	θ	R_{exp}	R_{th}
0.6133	0.3465	180	0.719	0.75602
		135	0.657	0.71614
		90	0.549	0.62555
		45	0.547	0.55224
		0	0.548	0.53048
	0.686	180	0.970	0.99319
		135	0.813	0.90817
		90	0.707	0.71096
		45	0.581	0.58945
		0	0.558	0.58829
0.4235	0.3465	180	0.777	0.78260
		135	0.744	0.76181
		90	0.718	0.71926
		45	0.705	0.69016
		0	0.729	0.68278
	0.686	180	0.903	0.92851
		135	0.804	0.87648
		90	0.750	0.77613
		45	0.728	0.73250
		0	0.741	0.73619

Note: Waves approach from $\theta = 180°$

moment. The pressure damping in the sea bed as ka increases, clearly has the effect of decreasing the force and moment with respect to what approximate theories would predict. This is consistent with what intuitive consideration would suggest but a quantitative rather than qualitative statement about the uplift force and overturning moment is quite important for design purposes. As an example for ka = 1, the force is about 50% smaller than that which simple approximate theories would predict.

Although not presented here in detail, additional studies led to the following conclusion: From the standpoint of minimizing the net uplift force and net overturning moment exerted on a cylinder of given radius b, also taking into account the effect of the pressure distribution along the upperside of the extended base, it appears that a cylinder without an extended base (a = b) rather than one with an extended base (a > b) is preferable. In the latter case one might have expected the dynamic pressure exerted along the upperside of the extended base to somehow compensate for the increase in the underside contribution from the dynamic seepage. But this was not the case. In other words, to minimize the force and moment, other considerations aside, an extended base should be avoided.

Insofar as an extended base does not remove the seepage velocity singularity occurring around the edge of the cylinder base such a base has little or no value in preventing erosion. Rather the technique of laying a rock filter around the cylinder base would seem more appropriate because it stabilizes the sand, while not increasing the net uplift force and overturning moment on the structure itself. The specific area to be protected around the cylinder base should be determined by calculating the exit gradient. As an example of what Eqs. 12 and 33 can provide, a contour of value 2.0 for the ratio of the hydraulic gradient amplitude to its value if no cylinder were there, namely of the coefficient $S(r,\theta)$, is shown on Fig. 6. Obviously for practical purposes, the critical exit gradient corresponding to the conditions of a specific problem should be determined and thus a critical contour around the cylinder base could be drawn, delimiting the area to be protected. As usual a safety factor should be introduced.

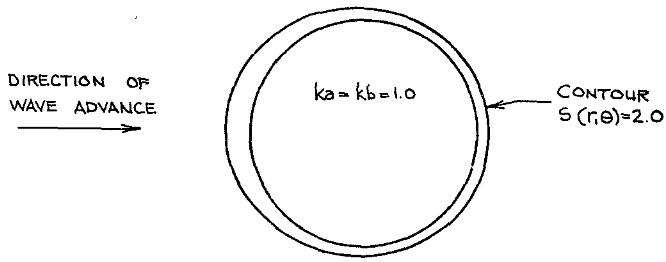

Fig. 6. Hydraulic Gradient Ratio

Table II shows that good agreement was found between experimental and theoretical results. Possible reasons for the small but persistent discrepancies include experimental error, difficulty in achieving a truly isotropic and homogeneous sand bed, and compressibility effects in the porous medium. In general these effects were not very significant.

CONCLUSIONS

1. The theory presented allows calculation of seepage pressure, uplift force and overturning moment values for a single vertical circular cylinder resting on a bed of sand of infinite depth. Evaluation of the exit gradient around the cylinder base is also possible. The nature of the seepage velocity singularity is shown to be similar to the singularity encountered at the toe of an impervious dam.

2. Normalized forms of the force and moment appear to be universal functions of two non-dimensional parameters ka and kb (k is the wave number, b the cylinder radius, and a the radius of the cylinder base), reducing to one when a = b. Graphs for these functions are provided so that once the physical characteristics of the problem are known, little additional computation is required.

3. A cylinder base extending beyond the cylinder radius does not remove the exit gradient singularity at the edge of the base. Furthermore, for a given cylinder radius, the effect of an extended base is to increase the maximum value of the net uplift force and overturning moment exerted on the cylinder. As a preferred protection against possible piping below and around the structure foundation, the use of a rock filter is recommended.

4. The theoretical results for the pressure appear to be in good agreement with data from a limited experimental program in a wave tank at the Hydraulics Laboratory of the University of Wisconsin-Madison.

5. The graphs presented in Fig. 2 show that approximate theories generally can not predict the wave-induced seepage effects on the cylinder.

ACKNOWLEDCMENTS

This material is based upon work supported by the National Science Foundation under Grant #ENC77-20030. Support was also provided by the Graduate School of the University of Wisconsin.

The writers are grateful to Professor Ben. Noble for his advice on dual integral equations, to Mr. R. Hughes for his technical assistance and to Mrs. R. Wyss for assistance in preparing the manuscript.

REFERENCES

1. Biot, M. A. (1941), "General Theory of Three Dimensional Consolidation", Journal of Applied Physics, Vol. 12, pp 155-164.

2. Dean, R. G. and D. R. F. Harleman (1966), "Interaction of Structures and Waves", chapter 8 of Estuary and Coastlines Hydrodynamics, Ippen (Editor), McGraw Hill Book Co., New York, N.Y.

3. Durand, T. J. P. (1978), Wave-Induced Seepage Effects on a Single Vertical Circular Cylinder Resting on a Bed of Sand, unpublished Independent Study Report, Department of Civil and Environmental Engineering, University of Wisconsin-Madison.

4. MacCamy, R. C. and R. A. Fuchs (1954), "Wave Forces on Piles: A Diffraction Theory", Technical Memorandum No. 69, U.S. Army Coastal Engineering Research Center (formerly Beach Erosion Board).

5. Madsen, O. S. (1978), "Wave-Induced Pore Pressures and Effective Stresses in a Porous Bed", Ceotechnique, Vol. 28, No. 4, pp 373-393.

6. Moshagen, J. and P. L. Monkmeyer (1979), "Wave-Induced Seepage Forces on Embedded Offshore Structures", Proc. Civil Eng. in the Oceans/IV Conf., San Francisco, Cal.

7. Moshagen, J. and A. Tørum (1975), "Wave-Induced Pressures in Permeable Sea Beds", Journal of the Waterways, Harbors and Coastal Engineering Division, Proc. ASCE, Vol. 101, No. WW1, Feb. 1975.

8. Putnam, J. A. (1949), "Loss of Wave Energy due to Percolation in a Permeable Sea Bottom", Trans. A.C.U., Vol. 30, No. 3, June 1949.

9. Sleath, J. F. A. (1970), "Wave-Induced Pressures in Beds of Sand", Journal of the Hydraulics Division, Proc. ASCE, Vol. 96, No. HY2, Feb. 1970.

10. Sneddon, I. N. (1966), Mixed Boundary Value Problems in Potential Theory, North Holland Publishing Company.

11. Spring, B. H. and P. L. Monkmeyer (1975), "Interaction of Plane Waves with a Row of Cylinders", Proc. Civil Engineering in the Oceans/III Conf., Newark, Delaware.

12. Watson, G. N. (1966), A Treatise on the Theory of Bessel Functions, Cambridge University Press.

13. Yamamoto, T. (1977), "Wave-Induced Instability in Seabeds", Coastal Sediments '77, ASCE, Charleston, South Carolina, Nov. 1977.